

*In Part 1 the connexion between the error of a cryo-current comparator and the magnetic field attenuation in the gap region of its superconducting shield has been treated for the special but very common case of co-axial gap regions. This paper extends the error analysis on gaps forming a ring cavity. Such gap elements occur in toroidal cryo-current comparators as a link between two adjacent co-axial cavities. The results for these comparators are: the only field component which may penetrate the gap without attenuation is the one containing the useful signal about the current linkage of the comparator. All other field components contribute to the error of the comparator. They are attenuated according to their degree of symmetry. As the exact way the error functions is known it will be possible to construct cryo-current comparators with a predictable upper limit to their dc error.*

## Field attenuation as the underlying principle of cryo-current comparators

### 2. Ring cavity elements

K. Grohmann, H.D. Hahlbohm, D. Hechtfisher, and H. Lübbig

Cryo-current comparators (CCCs) are devices in which the ratio of two currents flowing in the ratio windings can be determined with very high accuracy. The characteristic element of a CCC is a superconducting shield between the ratio windings and the detector, either a SQUID or a flux transformer coupled to a SQUID. The shields can be constructed in a variety of ways.<sup>1-4</sup> Common to all types is a gap region which prevents the signal short circuiting. From a former investigation<sup>5</sup> (Part 1 of this paper) we know that the attenuation of magnetic fields in this gap region is the key to the understanding of the error behaviour of a CCC. Up to now calculations had been performed for the cylindrical gap region which is a shielding element common to all known types of CCCs.

An exponential attenuation law has been found in which the attenuation factor is determined by the degree of field symmetry and by the geometrical parameters of the gap. The only field contribution which remains undamped in the gap region is the field containing the information about the net current linkage, that is the useful signal of a CCC.

It is the intention of the present paper to extend the calculations to gap regions forming ring cavities. These gap elements are necessary as a link between the two adjacent co-axial cavities in toroidal shielding systems of CCCs (Fig. 1).

In the theoretical part the field attenuation in isolated ring cavities is calculated. In the experimental part the combination co-axial cavity-ring cavity-co-axial cavity is investigated using an electrolytic tank. Finally, error measurements on a CCC consisting of pure ring cavities in series are reported.

#### Theory

The arrangement to be discussed is shown in Fig. 2. A superconducting ring cavity of inner radius  $r_1$  and outer

The authors are with the Physikalisch-Technische Bundesanstalt, Institut Berlin, Abbestr 2-12, 1000 Berlin 10, Germany. Received 9 July 1976.

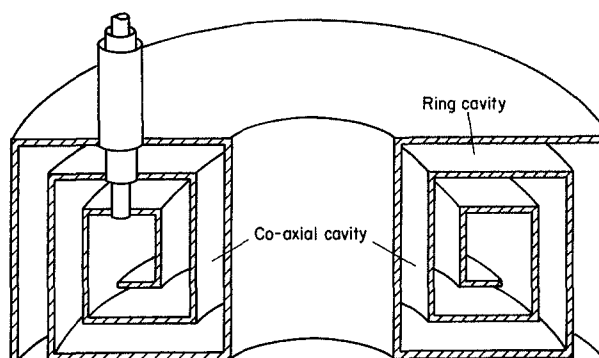


Fig. 1 Toroidal CCC with two types of cavities

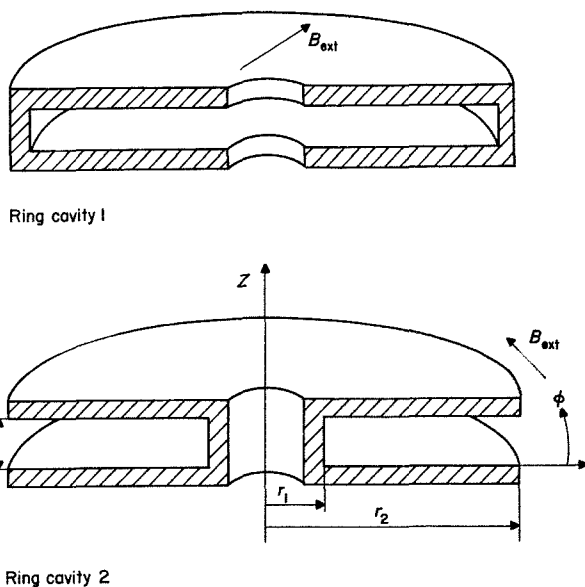


Fig. 2 Two types of ring cavities

radius  $r_2$  is formed by circular disks, the opening of the cavities being either at the inner or outer perimeter. In the space outside the cavities the magnetic field  $\mathbf{B}_{\text{ext}}$  is applied whose penetration into the cavities will be investigated.

The mathematical description we are using is the same as that used in Part 1. The scalar potential  $V$  is related to the magnetic field  $\mathbf{B}$  by

$$\mathbf{B} = -\nabla V \quad (1)$$

Outside the superconducting walls  $V$  obeys the Laplace equation

$$\nabla^2 V = 0 \quad (2)$$

The superconductivity of the walls of the ring cavities is introduced by postulating ideal diamagnetic behaviour. This demands the vanishing of all magnetic normal components at the superconducting surfaces, that is

$$\frac{\partial V}{\partial n} = 0 \quad (3)$$

where  $\partial/\partial n$  denotes the derivation with respect to the normal of the surface.

### Solution of the Laplace equation for ring cavities

Using cylindric coordinates and

$$V(\rho, \phi, z) = R(\rho)\Phi(\phi)Z(z)$$

we get the following solutions of the Laplace equation,<sup>6</sup> which are connected by two separation parameters  $n$  and  $k$

$$\Phi(\phi) = \begin{cases} A\phi + B & n = 0 \quad (4a) \\ A_n \sin(n\phi + \delta_n) & n > 0 \quad (4b) \end{cases}$$

$$Z(z) = \begin{cases} Cz + D & k = 0 \quad (5a) \\ C_k \sin(kz) + D_k \cos(kz) & k > 0 \quad (5b) \end{cases}$$

$$R(\rho) = \begin{cases} E \ln \rho + F & n = 0 \quad k = 0 \quad (6a) \\ E_n^0 \rho^n + F_n^0 \rho^{-n} & n > 0 \quad k = 0 \quad (6b) \\ E_n^k I_n(k\rho) + F_n^k K_n(k\rho) & n \geq 0 \quad k > 0 \quad (6c) \end{cases}$$

where  $I_n$  and  $K_n$  denote modified Bessel functions of the first and second kind, respectively and of integer order. (The occurrence of the modified Bessel-functions in contrast to Part 1 is demanded here by the special boundary conditions under consideration.)

The general solution for  $V$  is obtained by summing up the combinations of  $R$ ,  $\Phi$ , and  $Z$  for all possible values  $n$  and  $k$ . These values must be determined together with the coefficients  $A \dots F$  by means of the boundary conditions.

The symmetry of the external field  $\mathbf{B}$  determines the symmetry of the solution and thus the related values of  $n$ . If we allow an axial current  $I$  to flow in the region  $\rho < r_1$  we get  $ADF = -\mu_0 I/2\pi$  from Ampere's law. The boundary condition (3) applied to the superconducting planes  $z = 0$  and  $z = h$  leads to the result  $C = C_k = 0$  and furthermore the restriction that  $k$  can only assume the values

$$k = m \frac{\pi}{h} \quad m = 1, 2, 3 \dots \quad (7)$$

The same boundary condition (3) gives for the bottom of the cavities  $\rho = r_b$  ( $r_b = r_2$  for ring cavity 1 and  $r_b = r_1$  for ring cavity 2)

$$\frac{\partial V}{\partial \rho} = \frac{\partial R}{\partial \rho} = 0 \text{ at } \rho = r_b \quad (8)$$

resulting in

$$E = 0 \quad (9a)$$

$$F_n^0 = E_n^0 r_b^{2n} \quad (9b)$$

$$F_n^k = -E_n^k \frac{I_n'(kr_b)}{K_n'(kr_b)} \quad n = 0, 1, 2 \dots \quad (9c)$$

Taking into account all these results we get the following complete solution for the potential on the inside of the cavity

$$V(\rho, \phi, z) = V(n=0, k=0) + V(n=0, k>0) + V(n>0, k=0) + V(n>0, k>0) \quad (10)$$

with

$$V(n=0, k=0) = -\frac{\mu_0 I}{2\pi} \quad (11)$$

$V(n>0, k=0)$

$$= \sum_{n=1}^{\infty} E_n^0 (\rho^n + r_b^{2n} \rho^{-n}) A_n \sin(n\phi + \delta_n) \quad (12)$$

$$V(n=0, k>0) = \sum_{m=1}^{\infty} D_m \cos\left(\frac{m\pi z}{h}\right) E_0^m \left[ I_0\left(\frac{m\pi\rho}{h}\right) - \frac{I_0'(m\pi r_b/h)}{K_0'(m\pi r_b/h)} K_0\left(\frac{m\pi\rho}{h}\right) \right] \quad (13)$$

$V(n>0, k>0)$

$$= \sum_{m=1}^{\infty} \sum_{n=1}^{\infty} D_m \cos\left(\frac{m\pi z}{h}\right) A_n \sin(n\phi + \delta_n) \times E_n^m \left[ I_n\left(\frac{m\pi\rho}{h}\right) - \frac{I_n'(m\pi r_b/h)}{K_n'(m\pi r_b/h)} K_n\left(\frac{m\pi\rho}{h}\right) \right] \quad (14)$$

The first potential term  $V(n=0, k=0)$  is the only one without any  $\rho$ -dependence, resulting in an azimuthal field

$$B_\phi = -\frac{1}{\rho} \frac{\partial V}{\partial \phi} = +\frac{\mu_0 I}{2\pi\rho}$$

which provides information about the current linkage in the inner of the ring cavity independent of the special position of the exciting current carrying wire.

To calculate the total field within the cavity we have to determine all remaining constants in (12)-(14) by adapting these solutions to the given external potential at the entrance  $\rho = r_e$  of the cavity, which may be developed into a Fourier series

$$V_{\text{ext}}(r_e, \phi, z) = \sum_{n=1}^{\infty} V_n(r_e, z) \sin(n\phi + \delta_n) \quad (15)$$

where the 'modes'  $n$  describe the symmetry of our problem. We can avoid this troublesome way of finding the total solution since we are only interested in the  $\rho$ -dependence of the fields, that is, in the attenuation which the external fields undergo during intrusion into the cavity.

Because in our cryo-current comparator the measured quantity is the flux resulting from the azimuthal field, we only consider here the component

$$B_\phi = -\frac{1}{\rho} \frac{\partial V}{\partial \phi} \quad (16)$$

The form of the solutions (12)–(14) shows that each mode  $n$  of the external field has an own  $\rho$ -dependence. Therefore, we define an attenuation  $A^{(n)}$  for each mode  $n$  as the fraction:

$$A^{(n)} = \frac{B_\phi^{(n)}(\text{within the cavity})}{B_\phi^{(n)}(\text{entering the cavity})} \quad (17)$$

(It can be shown by a more detailed analysis that the attenuation of the  $B_\rho$  component shows similar results, whereas the  $B_z$  component may be neglected).

#### Attenuation for fields without z-dependence

Equation 12 describes the only solution which is dependent on  $\rho$  but independent of  $z$ . We obtain for the mode  $n$

$$B_\phi^{(n)} = -\frac{1}{\rho} \frac{\partial V^{(n)}}{\partial \phi} \sim \rho^{n-1} + r_b^{2n} \rho^{-n-1} \quad (18)$$

If we denote the radius of the entrance to the cavity by  $r_e$  we obtain from (17)

$$A^{(n)}(\rho) = \left(\frac{\rho}{r_e}\right)^{n-1} \frac{1 + (r_b/\rho)^{2n}}{1 + (r_b/r_e)^{2n}} \quad (19)$$

Distinguishing the two cases

$$\text{ring cavity 1: } r_e = r_1 \quad r_b = r_2 \quad (20a)$$

$$\text{ring cavity 2: } r_e = r_2 \quad r_b = r_1 \quad (20b)$$

we get

$$A_{rc1}^{(n)}(\rho) = \left(\frac{r_1}{\rho}\right)^{n+1} \frac{1 + (\rho/r_2)^{2n}}{1 + (r_1/r_2)^{2n}} \quad (21a)$$

$$A_{rc2}^{(n)}(\rho) = \left(\frac{\rho}{r_2}\right)^{n-1} \frac{1 + (r_1/\rho)^{2n}}{1 + (r_1/r_2)^{2n}} \quad (21b)$$

The lowest mode  $n = 1$  gives the lowest attenuation. Because  $r_1/r_2 < 1$  and  $r_1/\rho < 1$  the attenuation in the ring cavity 1 is always less than 1. But in the ring cavity 2 we obtain for  $n = 1$   $A_{rc2}^{(1)} > 1$ , that is, a slight increase of the field into the interior. For the higher modes we find again a field attenuation  $A_{rc2} < 1$ . For the first five modes with  $r_2/r_1 = 2$  and  $\rho = r_b$  Table 1 is obtained.

We see the ring cavity 2 is less effective in attenuating magnetic fields. Its main function in cryo-current comparators is to interconnect two adjacent co-axial cavities (see Fig. 1).

#### Attenuation of z-dependent fields

All terms with combined  $z$  and  $\rho$  dependences contain modified Bessel functions. In all real cryo-current comparators we have  $\rho/h > 10$  and therefore it follows  $x = m\pi\rho/h > 30$ . Then we may use the asymptotic representations

$$I_n(x) \approx e^x (2\pi x)^{-1/2} \quad (22a)$$

$$K_n(x) \approx e^{-x} \left(\frac{\pi}{2x}\right)^{1/2} \quad (22b)$$

which are independent of the order  $n$ . Therefore, the resultant radial dependence of the azimuthal field components is the same for all symmetry types, it depends only on the number  $m$  of extremes, the corresponding  $z$ -component has between the superconducting walls at  $z = 0$  and  $z = h$

$$B_\phi^{(n,m)} = -\frac{1}{\rho} \frac{\partial V^{(n,m)}}{\partial \phi} \approx \rho^{-3/2} [e^{(m\pi/h)\rho} + e^{(m\pi/h)(2r_b - \rho)}] \quad (23)$$

At the bottom of the cavity this results in an attenuation

$$A^{(m)}(\rho = r_b) = 2 \left(\frac{r_c}{r_b}\right)^{3/2} \left[ e^{(m\pi/h)(r_c - r_b)} + e^{(m\pi/h)(r_b - r_c)} \right]^{-1} \quad (24)$$

As in real CCCs  $|r_e - r_b| > 10h$  even with  $m = 1$  very strong attenuations of the order  $e^{-30} \approx 10^{-13}$  are obtained for a ring cavity 1 as well as for a ring cavity 2. Therefore we need not consider  $z$ -dependent fields further.

#### Attenuation by ring cavities followed by a co-axial cavity

In a CCC of the toroidal type (Fig. 1) a ring cavity of height  $h$  is followed by a co-axial cavity of width  $d$ . It would be very tedious to calculate the influence of this new boundary condition in a mathematically rigorous way. For our purpose, however, it will suffice to investigate this problem using certain simplifications.

As we have thin cavities, that is  $h, d \ll r_b$ , we can neglect any  $z$ -dependence in the ring cavity and any  $\rho$ -dependence in the following co-axial cavity. Furthermore, we know from our previous analysis that it is only necessary to consider the first mode of the corresponding potentials.

From this we obtain for the potential within the ring cavity

$$V_1^{rc} = D(E_1^0 \rho + F_1^0 \rho^{-1}) \sin \phi \quad (25)$$

and for the potential within the following co-axial cavity (see Part 1)

$$V_1^{cc} = C e^{-z/r_b} \sin \phi \quad (26)$$

We aim to determine the ratio of the coefficients  $E_1^0$  and  $F_1^0$  which contains information about the boundary at  $\rho = r_b$ . Using  $\nabla \cdot \mathbf{B} = 0$  and neglecting terms of order  $h/r_b \ll 1$ , it can be shown that the radial field component entering the corner region and the  $z$ -component leaving it are connected by

$$hB_\rho = \pm dB_z \quad (27)$$

Table 1. Attenuation for different modes  $r_2/r_1 = 2$

Mode	Ring cavity 1	Ring cavity 2
1	0.400	1.600
2	0.235	0.941
3	0.123	0.492
4	0.062	0.249
5	0.031	0.125

The plus and minus sign holds for ring cavity 1 and 2, respectively. From  $\nabla \times \mathbf{B} = 0$  it can be shown within the same degree of approximation that the azimuthal field component,  $B_\phi$ , remains unchanged while passing the corner, that is  $B_\phi^{cc} = B_\phi^c$ .

From these two relations we calculate, by means of the potentials given above, for a ring cavity 1

$$\frac{F_1^0}{E_1^0} = \frac{1 + d/h}{1 - d/h} r_2^2 \quad (28a)$$

and for a ring cavity 2

$$\frac{F_1^0}{E_1^0} = \frac{1 - d/h}{1 + d/h} r_1^2 \quad (28b)$$

If the width  $d$  of the co-axial cavity is zero, these formulas give the result (9b), found earlier for ring cavities closed at  $\rho = r_b$ . If the width of the co-axial cavity equals the height of the ring cavity, we obtain the interesting result, that the term proportional to  $\rho$  for ring cavity 1 and the term proportional to  $1/\rho$  for ring cavity 2 can be neglected, that is the influence of the cavity's bottom. For this case, which normally occurs in a CCC, the attenuation of the first mode by the two types of ring cavities is simply given by

$$A_{rc1}^1(\rho) = \left(\frac{r_1}{\rho}\right)^2 \quad (29a)$$

$$A_{rc2}^1(\rho) = \left(\frac{\rho}{r_2}\right)^0 = 1 \quad (29b)$$

To conclude, it should be mentioned that the same arguments will lead to the conclusion that the influence of the bottom of a co-axial cavity can be neglected, if it is followed by a ring cavity of equal width.

## Experiments

### Interconnection of co-axial and ring cavities

We have investigated the attenuation of combined co-axial and ring cavities by an experiment carried out in the electrolytic tank. An irrotational magnetic field  $\mathbf{B}$  was simulated by the electric field  $\mathbf{E}$ ; the magnetic field behaviour at superconducting surfaces  $\mathbf{B}_n = 0$  being analogous to the electric field behaviour at insulating surfaces  $\mathbf{E}_n = 0$ . The gap region between the isolators was filled with the electrolyte and an electrical ac field was injected at the entrance of the gap region by two probes displaced by  $180^\circ$  (thus injecting an entrance field with symmetry  $n = 1$ ). On the inside of the gap region the voltage between two moveable probes at a distance of 6 mm was measured. The results of these measurements are shown in Fig. 3. Here the attenuation factor, as defined in (17), is plotted as a function of the total length  $l$  of the gap region. The dots denote the measurements in the electrolytic tank. As the width of the co-axial cavity equals the height of the ring cavity the experimental results can be described by the approximation developed in the previous section. From Fig. 3 it can be clearly seen that the ring cavity 2 is ineffective for field attenuation while the ring cavity 1 shows an  $1/l^2$  dependence. This attenuation is for the special gap geometry investigated here quite comparable with the exponential attenuation of the adjacent short co-axial cavities.

### Cryo-current comparator consisting of pure ring cavities

To demonstrate the attenuation of pure ring cavities the special cryo-current comparator shown in Fig. 4 was constructed (Folder type CCC<sup>4</sup>). It consists of ring cavity elements which form the gap region; the widths of the rudimental co-axial links and the individual ring cavities being equal. The ratio windings (1 : 1 ratio) surround the comparators' shield at such a distance that the single ring cavity elements could be removed in turn without a change in the ratio windings' geometry. Fig. 5 shows the measured error of this comparator as function of the number of ring cavity elements. (The error  $e$  is defined according to

$$N_1 I_1 = N_2 I_2 (1 + e)$$

as the relative deviation of the current linkages if the output signal of the comparator is zero. It can be measured by injecting the nominal current  $I_1$  and  $I_2$  into the ratio windings and observing the output signal.) Because any removal of a ring cavity 1 element weakens the attenuation of the ratio windings' stray fields the error of the com-

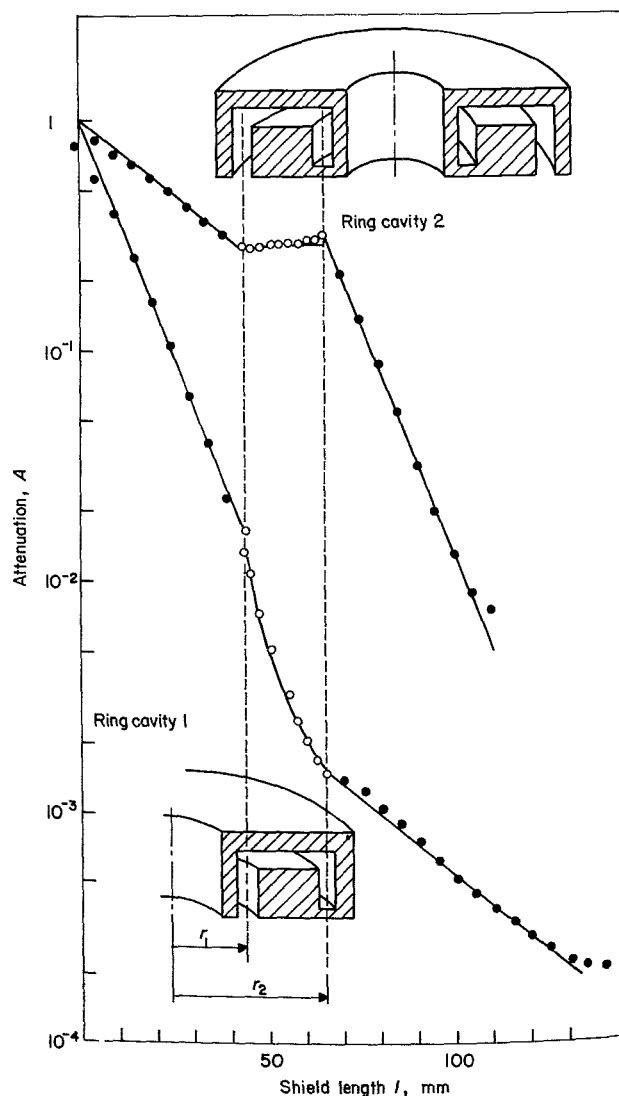


Fig. 3 Field attenuation  $A$  by the interconnection of co-axial and ring cavities as a function of the length of the gap ..... measured in the electrolytic tank, — calculated from (29a) and (29b)

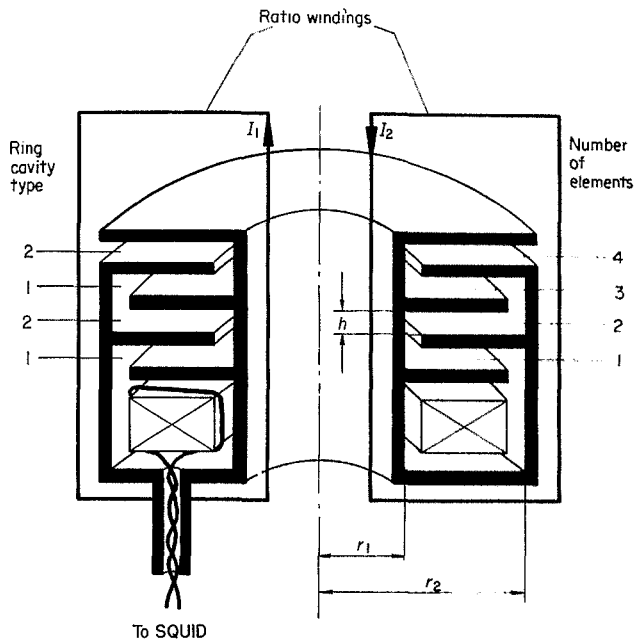


Fig. 4 Folder type comparator consisting of four ring cavities

parator is increased by this. The factor of this increase, as calculated from the geometry of the shield elements using (29), is 56, whereas the mean measured value is 60. The removal of a ring cavity 2 element does not effect the error behaviour as expected from the theory.

### Conclusion

The error of a cryo-current comparator depends on the degree of attenuation which external fields undergo in the gap region of the superconducting shield. While this has been proved in Part 1 for a co-axial gap geometry the studies described in this paper show the same both theoretically and experimentally for ring cavities too. Both cavity elements are sufficient to construct the established types of cryo-current comparators. Therefore, it is now possible by choice of the appropriate gap geometry to construct cryo-current comparators with a predictable upper limit to their dc errors.

The authors wish to thank Mr H.-J. Handke for the construction and measurement on the folder type CCC.

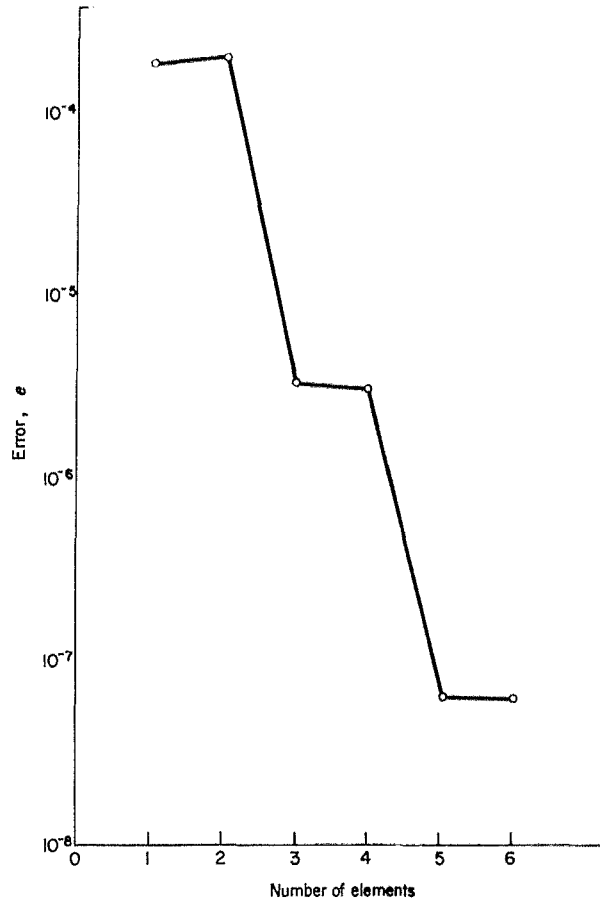


Fig. 5 Error of the folder type comparator as a function of the number of ring cavity elements

### References

- 1 Harvey, I.K. *Rev Sci Instr* 43 (1972) 1626
- 2 Grohmann, K., Hahlbohm, H.-D., Lübbig, H., Ramin, H. *PTB-Mitteilungen* 83 (1973) 313
- 3 Sullivan, D.B., Dziuba, R.F. *IEEE Trans Instr Meas* IM 23 (1974) 256
- 4 Grohmann, K., Hahlbohm, H.-D., Lübbig, H., Ramin, H. *IEEE Trans Instr Meas* IM 23 (1974) 261
- 5 Grohmann, K., Hahlbohm, H.-D., Hechtfisher, D., Lübbig, H. *Cryogenics* 16 (1976) 423
- 6 Smythe, W.R. *Static and Dynamic Electricity*, 3rd edn (McGraw-Hill, London)